Quality Improvement Study

Tradeoff between noise reduction and inartificial visualization in a model-based iterative reconstruction algorithm on coronary computed tomography angiography

Kenichiro Hirata, MD[a], Daisuke Utsunomiya, MD[a,*], Masafumi Kidoh, MD[a], Yoshinori Funama, PhD[b], Seitaro Oda, MD[a], Hideaki Yuki, MD[a], Yasunori Nagayama, MD[a], Yuji Iyama, MD[a], Takeshi Nakaura, MD[a], Daisuke Sakabe, RT[c], Kenichi Tsujita, MD[d], Yasuyuki Yamashita, MD[a]

Abstract

We aimed to evaluate the image quality performance of coronary CT angiography (CTA) under the different settings of forward-projected model-based iterative reconstruction solutions (FIRST).

Thirty patients undergoing coronary CTA were included. Each image was reconstructed using filtered back projection (FBP), adaptive iterative dose reduction 3D (AIDR-3D), and 2 model-based iterative reconstructions including FIRST-body and FIRST-cardiac sharp (CS). CT number and noise were measured in the coronary vessels and plaque. Subjective image-quality scores were obtained for noise and structure visibility.

In the objective image analysis, FIRST-body produced the significantly highest contrast-to-noise ratio. Regarding subjective image quality, FIRST-CS had the highest score for structure visibility, although the image noise score was inferior to that of FIRST-body.

In conclusion, FIRST provides significant improvements in objective and subjective image quality compared with FBP and AIDR-3D. FIRST-body effectively reduces image noise, but the structure visibility with FIRST-CS was superior to FIRST-body.

Abbreviations: AIDR-3D = adaptive iterative dose reduction 3D, CAD = coronary artery disease, CNR = contrast-to-noise ratio, CT = computed tomography, CTA = computed tomography angiography, FBP = filtered back projection, FIRST = forward-projected model-based iterative reconstruction solution, FIRST-B = forward-projected model-based iterative reconstruction solution–body, FIRST-CS = forward-projected model-based iterative reconstruction solution–cardiac sharp, IR = iterative reconstruction, RCA = right coronary artery, ROI = region of interest.

Keywords: atherosclerotic plaque, cardiac imaging, coronary artery disease, image reconstruction, multidetector computed tomography

1. Introduction

Coronary computed tomography angiography (CTA) is well established for the precise evaluation of coronary artery stenosis, and coronary CTA has an advantage beyond coronary angiography, that is, plaque characterization.[1,2] Newer-generation computed tomography (CT) modalities such as 256-slice,

320-detector, and dual-source, and newer iterative reconstruction (IR) techniques have been developed to improve the image quality of coronary CTA. Not only the stenosis severity but also plaque characterization is required for coronary CTA, leading to appropriate patient management.[2,3] High-risk CT imaging features, that is, low attenuation plaques (<30 HU), positive remodeling, spotty calcification, and the napkin-ring sign, are proposed in the standardized reporting guideline.[2] Therefore, it is crucial to balance image noise reduction and clear visibility of cardiac structures for the evaluation of coronary artery disease (CAD) during coronary CTA.[1,3]

The reconstruction techniques can alter the image quality and appearance of coronary CTA. The most traditional method for CT image reconstruction is filtered back projection (FBP), which is simple and rapid[4] but it is based on several assumptions of an ideal system such as the point source of a focal spot. Hybrid-type IR, which combines FBP with IR, is also widely used in clinical practice because it can effectively reduce quantum image noise within a clinically acceptable time, allowing for radiation dose reduction.[5–7] However, the system model is not considered, and the plaque CT number and the degree of stenosis may be inaccurate in the hybrid-type IR.[8] Most recently, model-based IR was developed, and it relies on optics, system, cone beam, and statistical noise models.[8–10] Veo (GE Healthcare, Waukesha, WI) and IMR (Philips Healthcare, Cleveland, OH) are examples of model-based IR.[10–12] Previous studies reported that the model-based IR drastically reduced image

noise of low-radiation-dose CT with preserved image quality.[10,11] Model-based IR iteratively minimizes the cost function; the process consists of 2 domains: the projection data and volume data (regularization). In simple terms, the projection data and volume data domains control the spatial resolution and image noise, respectively, giving rise to a tradeoff relationship between inartificial visualization and noise reduction.[12–14] The forward-projected model-based IR solution (FIRST) technique was developed as a model-based IR by Canon Medical Systems, and it has 2 types of IR settings for coronary CTA: FIRST "body" (FIRST-B) and FIRST "cardiac sharp" (FIRST-CS) settings, focusing on noise reduction and spatial resolution, respectively.[8,9,15] Previous studies have suggested that the CT image quality under a model-based IR algorithm may be affected by several factors, including contrast, radiation dose, and lesion size.[12,14,16] However, a detailed analysis to compare the different model-based IR algorithms has not been reported previously, and the question of whether the model-based IR should focus on inartificial visualization or noise reduction remains unclear on coronary CTA. We hypothesized that the model-based IR can be used for improvement of cardiac structure visibility instead of radiation dose reduction. Thus, we investigated the objective and subjective visualization performance of the model-based IR for 320-detector row coronary CTA by comparing the image quality among FBP, hybrid-type IR, and 2 model-based IR techniques (FIRST-B and FIRST-CS).

2. Methods

This retrospective study was approved by our ethics committee (approve number, #1287), and the required informed consent was waived.

2.1. Patients

We reviewed data for 32 patients with non-calcified or predominantly non-calcified plaques and moderate stenosis (50%–70%) on electrocardiogram-gated coronary CTA between June 2016 and September 2016. Two patients (1 with inadequate breath-holding during scanning and 1 with atrial fibrillation) were excluded. Consequently, 30 patients (11 women; mean age, 66 ± 14 years; age range, 32–91 years) were included. All patients were referred for coronary CTA for clinical reasons based on published guidelines.[17]

2.2. Coronary CTA protocol

All coronary CTA studies were performed using a 320-detector row CT scanner (Aquilion ONE GENESIS, Canon Medical Systems, Otawara, Japan). The parameters for CT scanning were as follows: prospective ECG-gating axial scans; 320 rows × 0.5-mm collimation; rotation time, 275 ms; tube voltage, 120 kV; and tube current, 220 to 300 mA (automatic exposure control). A beta-blocker (20 mg, Lopressor; Novartis Pharma, Tokyo, Japan) was orally administered 1 hour before coronary CTA scanning. If the heart rate exceeded 65 bpm in the CT suite, the beta-blocker landiolol hydrochloride (6–10 mg, Corebeta; Ono Pharmaceutical, Osaka, Japan) was intravenously administered 5 minutes before coronary CTA scanning. Each patient received 0.3 mg of nitroglycerin sublingually 5 to 10 minutes before scanning to dilate the coronary arteries.

For coronary CTA, contrast material (iodine concentration 370 mg/mL; Iopamiron 370; Bayer HealthCare, Osaka, Japan) was administered to each patient via a 20-gauge catheter inserted into an antecubital vein using a double-head power injector (Dual Shot GX-7; Nemoto Kyorindo, Tokyo, Japan). The amount of contrast material, adjusted to the body weight of each patient (300 mL/kg), was injected over a fixed injection duration of 12 seconds. We then injected 40 mL of a normal saline solution at the same rate as the contrast material. The start time of data acquisition was determined by a computer-assisted bolus-tracking program. The trigger threshold was set at 250 HU for the ascending aortic region of interest (ROI). Six seconds after the trigger, CT data acquisition was started.

Furthermore, we estimated the effective radiation dose of the chest with the following equation: effective dose = (CTDI$_{vol}$ × anatomical range for the chest) × 0.014.[13]

2.3. Image reconstruction

Four images were generated for each patient during the mid-diastolic phase, using the following reconstruction techniques: FBP, hybrid-IR (adaptive iterative dose reduction 3D [AIDR-3D]), and 2 model-based IRs (FIRST-B and FIRST-CS). Cross-sectional images were reconstructed with a section thickness of 0.5 mm in 0.25-mm increments. Multiplanar and curved planar reconstruction images were reconstructed.

Table 1

Mean CT number, noise, and CNR of the coronary vessel and plaque.

	Reconstruction technique				
	FBP	AIDR-3D	FIRST-B	FIRST-CS	*P*-value
Proximal vessel					
CT number	425.2 ± 63.4	416.6 ± 60	424.9 ± 67.2	432.7 ± 63.9	.78
CNR	10.5 ± 2.3	17.8 ± 4.7	46.3 ± 18.6	22.3 ± 4.3	<.01
Distal vessel					
CT number	323.3 ± 59.5	284.5 ± 86.5	293.5 ± 100.0	328.1 ± 92.4	.16
CNR	4.7 ± 1.9	7.2 ± 3.7	20.0 ± 11.9	11.5 ± 5.3	<.01
Septal branch					
CT number	281.7 ± 82.0	256.4 ± 58.0	236.2 ± 68.3	271.0 ± 67.1	.04
CNR	4.0 ± 1.3	6.1 ± 2.5	13.5 ± 7.8	7.8 ± 5.6	<.01
Plaque					
CT number	111.0 ± 68.1	106.8 ± 66.0	114.4 ± 67.0	106.3 ± 57.0	.95
CNR	3.9 ± 1.5	6.8 ± 2.9	17.2 ± 11.1	8.0 ± 3.0	<.01

AIDR-3D = adaptive iterative dose reduction 3D, CNR = contrast to noise ratio, CT = computed tomography, FBP = filtered back projection, FIRST-B = forward-projected model-based iterative reconstruction–body, FIRST-CS = forward-projected model-based iterative reconstruction–cardiac sharp.

Table 2

Multiple comparisons of CNR values among the 4 reconstruction techniques.

	Reconstruction	P-value
Proximal vessel	FBP vs AIDR-3D	<.05
	FBP vs FIRST-B	<.01
	FBP vs FIRST-CS	<.01
	AIDR-3D vs FIRST-B	<.01
	AIDR-3D vs FIRST-CS	NS
	FIRST-B vs FIRST-CS	<.01
Distal vessel	FBP vs AIDR-3D	NS
	FBP vs FIRST-B	<.01
	FBP vs FIRST-CS	<.01
	AIDR-3D vs FIRST-B	<.01
	AIDR-3D vs FIRST-CS	NS
	FIRST-B vs FIRST-CS	<.01
Septal branch	FBP vs AIDR-3D	NS
	FBP vs FIRST-B	<.01
	FBP vs FIRST-CS	<.01
	AIDR-3D vs FIRST-B	<.01
	AIDR-3D vs FIRST-CS	NS
	FIRST-B vs FIRST-CS	<.01
Plaque	FBP vs AIDR-3D	NS
	FBP vs FIRST-B	<.01
	FBP vs FIRST-CS	<.05
	AIDR-3D vs FIRST-B	<.01
	AIDR-3D vs FIRST-CS	NS
	FIRST-B vs FIRST-CS	<.01

AIDR-3D = adaptive iterative dose reduction 3D, CNR = contrast to noise ratio, FBP = filtered back projection, FIRST-B = forward-projected model-based iterative reconstruction- body, FIRST-CS = forward-projected model-based iterative reconstruction- cardiac sharp.

2.4. Quantitative evaluation

All image series were transferred to a workstation (Ziostation 2, Ziosoft Inc., Tokyo, Japan) for image analysis. The mean CT number, image noise, and contrast-to-noise ratio (CNR) were used as objective image quality parameters. The CT number was obtained by placing circular ROIs in the proximal and distal parts of the right coronary artery (RCA), main septal branch, coronary plaque, and perivascular fat by the consensus of 2 board-certified radiologists. ROIs of 5 to 7 and 1.5 to 2.5 mm^2, which were selected to be of sufficient size to not be affected by pixel variability or approach the contours of the vessel, were selected for the proximal and distal vessels, respectively. The measurements of ROIs for different reconstruction images in each patient were performed using the copy–paste technique to mirror the identical ROIs on the FBP, AIDR-3D, FIRST-B, and FIRST-CS images. In addition, image noise was measured as the standard deviation of a manually placed circular ROI (approximately 200 mm^2) within the descending aorta at the same level. For the measurements in the coronary arteries, plaques, and perivascular fat, the size, shape, and position of ROIs were kept constant. We adopted the RCA as a representative coronary vessel because it runs from the top to the bottom of the heart, and it was considered that the relationship of the heart with vascular quantitative parameters could be properly evaluated. The septal branch was selected as a representative small vessel. Then, the CNRs of the vessel and the plaque were calculated as follows:
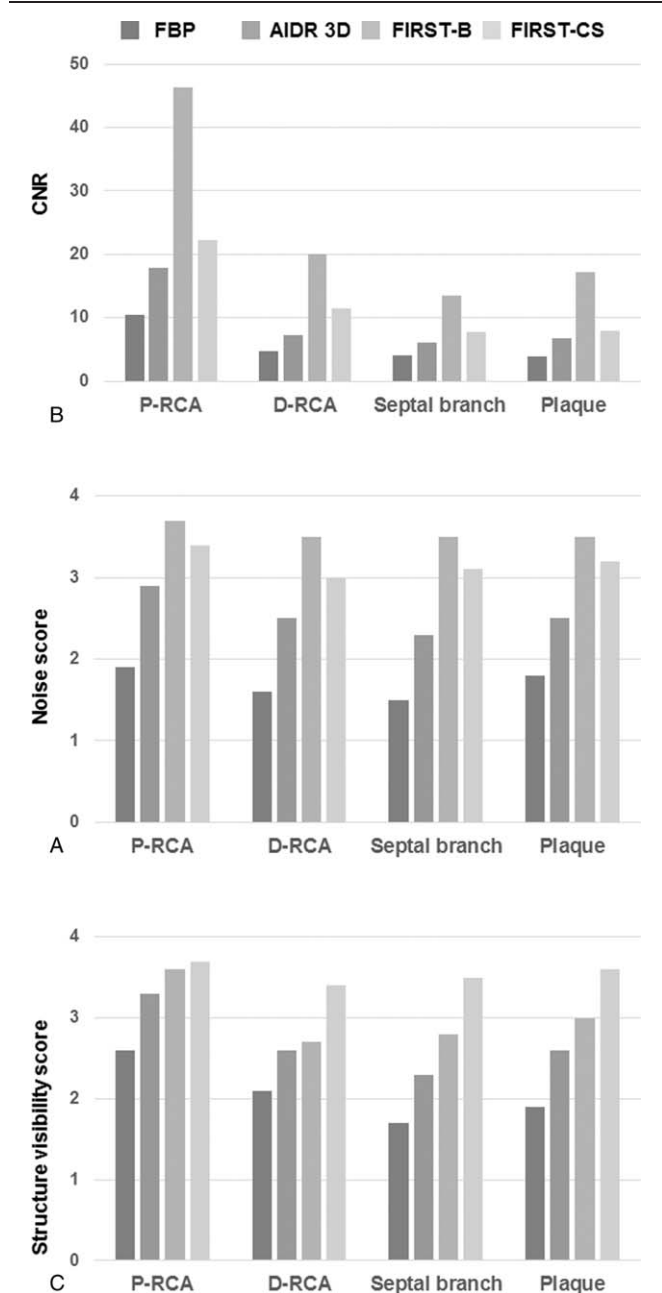

Figure 1. Results of the qualitative (A) and visual evaluation (B and C) of 4 reconstruction algorithms (FBP, AIDR-3D, FIRST-B, and FIRST-CS). A. Mean CNR was highest with FIRST-B in each structure. B. Visual score of image noise was significantly highest with FIRST-B. C. Visual score of structure visibility was significantly highest with FIRST-CS, especially in small structures. AIDR-3D = adaptive iterative dose reduction 3D, CNR = contrast-to-noise ratio, D-RCA = distal right coronary artery, FBP = filtered back projection, FIRST-B = forward-projected model-based iterative reconstruction solution–body, FIRST-CS = forward-projected model-based iterative reconstruction solution–cardiac sharp, P-RCA = proximal right coronary artery.

$$CNRvessel = \frac{(CT\ number\ of\ lumen - CT\ number\ of\ perivascular\ fat)}{image\ noise}$$

$$CNRplaque = \frac{(CT\ number\ of\ plaque - CT\ number\ of\ perivascular\ fat)}{image\ noise}$$

Table 3

Interobserver agreement (kappa) for the visual evaluation scores (image noise and structure visibility) of the coronary vessels and plaque.

	Reconstruction technique			
	FBP	AIDR-3D	FIRST-B	FIRST-CS
Proximal vessel				
Noise	0.479	0.589	0.586	0.528
Visibility	0.552	0.684	0.684	0.516
Distal vessel				
Noise	0.569	0.732	0.588	0.833
Visibility	0.608	0.651	0.727	0.798
Septal branch				
Noise	0.533	0.571	0.667	0.930
Visibility	0.726	0.633	0.847	0.733
Plaque				
Noise	0.641	0.796	0.802	0.793
Visibility	0.739	0.675	0.869	0.714

AIDR-3D = adaptive iterative dose reduction 3D, FBP = filtered back projection, FIRST-B = forward-projected model-based iterative reconstruction- body, FIRST-CS = forward-projected model-based iterative reconstruction- cardiac sharp.

2.5. Qualitative evaluation

All images were interpreted on an image processing workstation (Ziostation 2, Ziosoft, Tokyo, Japan) by 2 board-certified radiologists with 13 and 7 years of cardiac CT experience, respectively. Disagreement between the 2 observers was settled, and the final visual score was determined by a consensus review that included a third senior radiologist with 33 years of experience in cardiovascular imaging. Images including transverse source, multiplanar reconstruction, and thin-slab (2-mm) maximum-intensity projection images at a window level of 200 HU and a width of 800 HU were available for the visual evaluation. Images with the 4 different reconstructions (FBP, AIDR-3D, FIRST-B, FIRST-CS) were intermixed, and the observers were blinded to the reconstruction technique used and the identities of the patients.

The observers independently performed visual evaluation of the image noise (grainy and speckled appearance) and structure visibility (image texture and sharpness). The image noise of the proximal and distal parts of the RCA was graded on a 4-point

Table 4

Visual evaluation scores (image noise and structure visibility) of the coronary vessels and plaques.

	Reconstruction technique				
	FBP	AIDR-3D	FIRST-B	FIRST-CS	P-value
Proximal vessel					
Noise	1.9 ± 0.5	2.9 ± 0.5	3.7 ± 0.5	3.4 ± 0.6	<.001
Visibility	2.6 ± 0.5	3.3 ± 0.6	3.6 ± 0.6	3.7 ± 0.5	<.001
Distal vessel					
Noise	1.6 ± 0.5	2.5 ± 0.5	3.5 ± 0.5	3.0 ± 0.5	<.001
Visibility	2.1 ± 0.5	2.6 ± 0.5	2.7 ± 0.5	3.4 ± 0.5	<.001
Septal branch					
Noise	1.5 ± 0.5	2.3 ± 0.6	3.5 ± 0.5	3.1 ± 0.5	<.001
Visibility	1.7 ± 0.7	2.3 ± 0.6	2.8 ± 0.8	3.5 ± 0.5	<.001
Plaque					
Noise	1.8 ± 0.6	2.5 ± 0.5	3.5 ± 0.5	3.2 ± 0.4	<.001
Visibility	1.9 ± 0.7	2.6 ± 0.5	3.0 ± 0.4	3.6 ± 0.5	<.001

AIDR 3D = adaptive iterative dose reduction 3D, FBP = filtered back projection, FIRST-B = forward-projected model-based iterative reconstruction- body, FIRST-CS = forward-projected model-based iterative reconstruction- cardiac sharp.

Table 5

Multiple comparisons of visual evaluation scores.

	Reconstruction	Image noise	Structure visibility
Proximal vessel	FBP vs AIDR-3D	S	S
	FBP vs FIRST-B	S	S
	FBP vs FIRST-CS	S	S
	AIDR-3D vs FIRST-B	S	S
	AIDR-3D vs FIRST-CS	S	S
	FIRST-B vs FIRST-CS	S	NS
Distal vessel	FBP vs AIDR-3D	S	S
	FBP vs FIRST-B	S	S
	FBP vs FIRST-CS	S	S
	AIDR-3D vs FIRST-B	S	NS
	AIDR-3D vs FIRST-CS	S	S
	FIRST-B vs FIRST-CS	S	S
Septal branch	FBP vs AIDR-3D	S	S
	FBP vs FIRST-B	S	S
	FBP vs FIRST-CS	S	S
	AIDR-3D vs FIRST-B	S	S
	AIDR-3D vs FIRST-CS	S	S
	FIRST-B vs FIRST-CS	S	S
Plaque	FBP vs AIDR-3D	S	S
	FBP vs FIRST-B	S	S
	FBP vs FIRST-CS	S	S
	AIDR-3D vs FIRST-B	S	S
	AIDR-3D vs FIRST-CS	S	S
	FIRST-B vs FIRST-CS	S	S

AIDR 3D = adaptive iterative dose reduction 3D, FBP = filtered back projection, FIRST-B = forward-projected model-based iterative reconstruction- body, FIRST-CS = forward-projected model-based iterative reconstruction- cardiac sharp, NS = not significant, S = significant.

scale (worst, 1; best, 4) as follows: 1 = marked grainy and speckled appearance; 2 = moderate speckled appearance; 3 = mild grainy and speckled appearance; and 4 = minimal to no grainy and speckled appearance. The structure visibility of the RCA, septal branch, and coronary plaque was graded as follows: 1 = major artificial appearance and unclear visibility; 2 = moderate artificial appearance and reduced visibility; 3 = mild artificial appearance and acceptable visibility; and 4 = inartificial appearance and good visibility.

2.6. Statistical analysis

Statistical analysis was performed using computer software (MedCalc version 17.2, MedCalc, Mariakerke, Belgium). Continuous variables (objective quantitative measurements) were compared using the Tukey–Kramer test. Ordinal variables (subjective imaging qualitative grading) were compared using the Friedman test, and pairwise multiple comparisons were performed using the Conover–Inman test. The degree of agreement between the 2 reviewers in the visual evaluations of image noise and structure visibility was measured using kappa statistics (kappa value of 0 = no agreement; >0–0.20 = poor agreement; 0.21–0.40 = fair agreement; 0.41–0.60 = moderate agreement; 0.61–0.80 = substantial agreement; and 0.81–0.99 = almost perfect agreement). A P-value of less than .05 was considered statistically significant.

3. Results

The mean volume CT dose index was 30.2 ± 15.9 mGy, and the mean DLP was 479.5 ± 261.9 mGy cm. The mean effective dose for the coronary CTA was 6.7 ± 3.6 mSv.
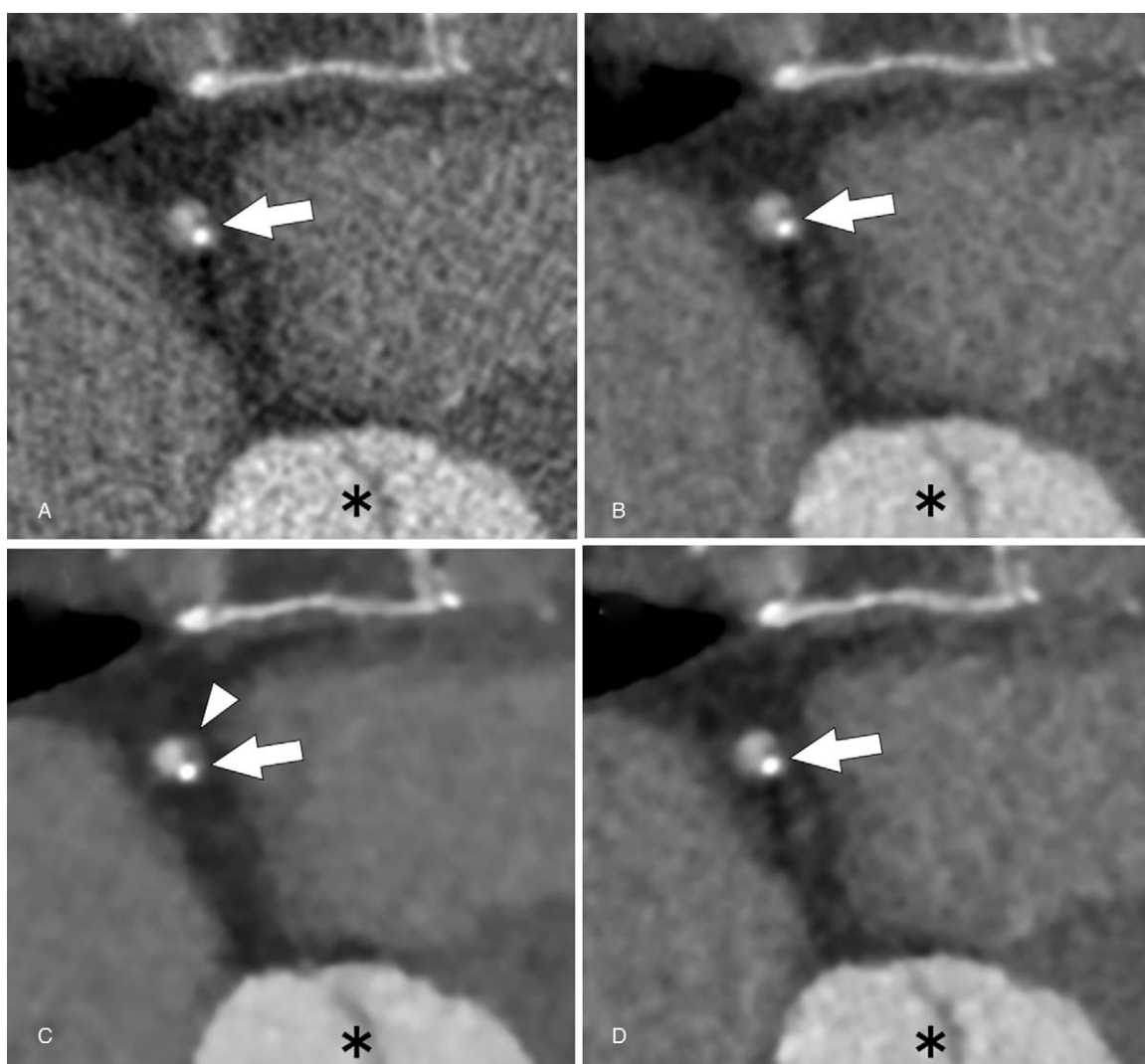
Figure 2. Axial coronary CT angiographic images of a 50-year-old woman with a partially calcified plaque (arrow) in the proximal right coronary artery under 4 reconstruction algorithms (A, FBP; B, AIDR-3D; C, FIRST-B; and D, FIRST-CS). FIRST images (C and D) shows lower noise compared with that of FBP (A) and AIDR3D images (B). However, FIRST-B shows artificial blooming of the plaque margin (C, arrowhead). FIRST-CS shows sharp plaque margin and inartificial appearance, Asterisk indicates aortic root. AIDR-3D = adaptive iterative dose reduction 3D, CNR = contrast-to-noise ratio, CT = computed tomography, D-RCA = distal right coronary artery, FBP = filtered back projection, FIRST-B = forward-projected model-based iterative reconstruction solution–body, FIRST-CS = forward-projected model-based iterative reconstruction solution–cardiac sharp, P-RCA = proximal right coronary artery.

3.1. Objective image quality evaluation

There were no significant differences in the CT number of the proximal coronary artery, distal coronary artery, and coronary plaque among the 4 reconstruction methods of FBP, AIDR-3D, FIRST-B, and FIRST-CS (Table 1). Regarding the septal branch (small vessel), the CT number was significantly lower for FIRST-B than for FBP (Table 1). The image noise values of the proximal RCA were 49.1 ± 8.8, 28.9 ± 7.2, 12.0 ± 3.6, and 23.5 ± 4.1 HU for FBP, AIDR-3D, FIRST-B, and FIRST-CS, respectively, and the differences were significant ($P < .01$). The corresponding noise values of the distal RCA were 55.2 ± 11.8, 30.1 ± 6.0, 11.7 ± 3.4, and 22.7 ± 5.1 HU ($P < .01$), respectively. FIRST-B produced significantly higher CNRs in the proximal and distal coronary vessels, septal branch, and coronary plaque (Tables 1 and 2, and Fig. 1A). Multiple comparison results of CNR are shown in Table 2.

3.2. Subjective image quality evaluation

The interobserver agreement (kappa) was moderate to substantial for coronary vessels with the 4 reconstructions techniques excluding that for image noise in the distal vessel with FIRST-CS (kappa = 0.833, almost perfect agreement) (Table 3). The interobserver agreement was higher for the septal branch and coronary plaque with FIRST than with FBP and AIDR-3D (Table 3).

The subjective image quality for image noise and structural visibility of coronary vessels and plaque was significantly higher with IR (AIDR-3D, FIRST-B, FIRST-CS) than with FBP (Tables 4 and 5). FIRST-B produced the highest score for image noise; conversely, FIRST-CS provided the highest score for structural visibility among the 4 reconstruction techniques (Fig. 1B and C). Representative cases are shown in Figs. 2–4.
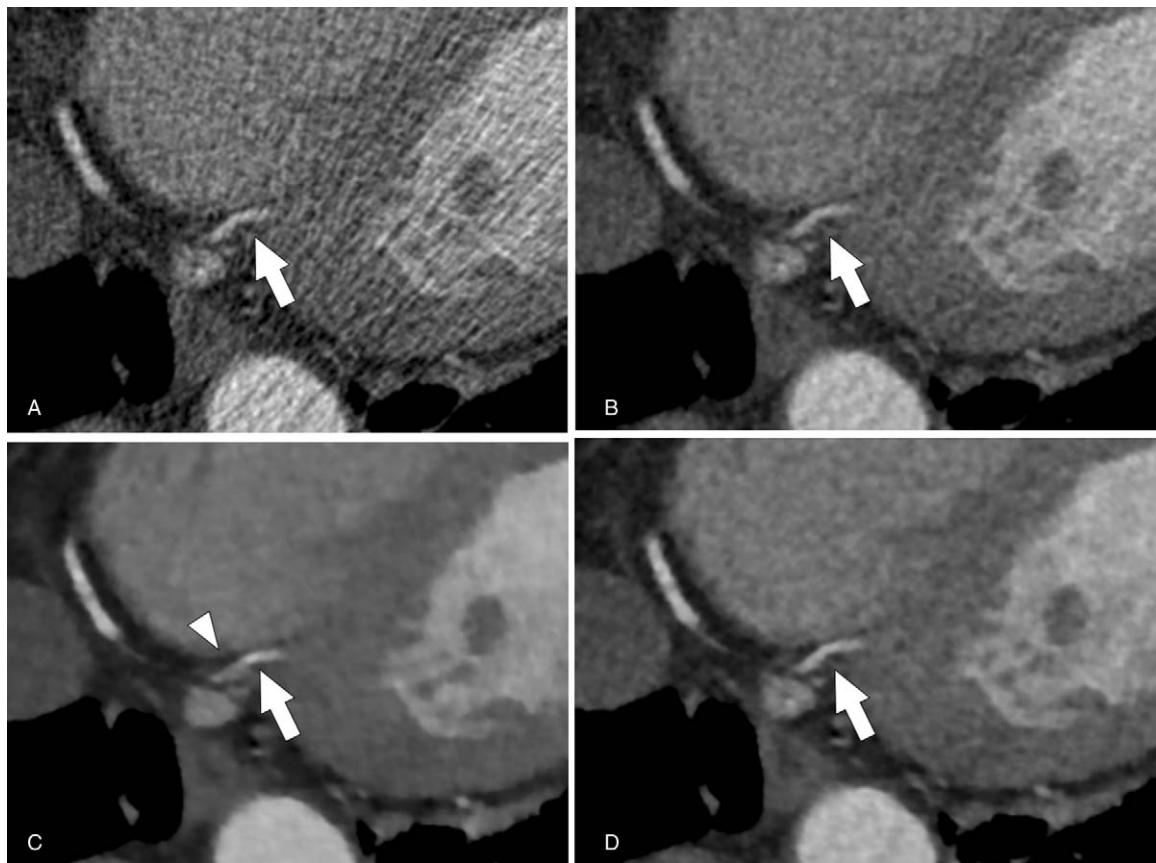
Figure 3. Axial coronary CT angiographic images of the normal distal right coronary artery (arrow) of a 67-year-old woman under 4 reconstruction algorithms (A, FBP; B, AIDR-3D; C, FIRST-B; and D, FIRST-CS). FIRST images (C and D) show lower noise compared with that of FBP (A) and AIDR-3D images (B). However, the vessel contour is partially obscured on the FIRST-B image (C, arrowhead). AIDR-3D = adaptive iterative dose reduction 3D, CNR = contrast-to-noise ratio, CT = computed tomography, D-RCA = distal right coronary artery, FBP = filtered back projection, FIRST-B = forward-projected model-based iterative reconstruction solution–body, FIRST-CS = forward-projected model-based iterative reconstruction solution–cardiac sharp, P-RCA = proximal right coronary artery.

4. Discussion

In the present study, we compared 4 coronary CTA reconstruction methods (FBP, AIDR-3D, FIRST-B, and FIRST-CS) for objective and subjective image quality, and uncovered the following findings: (1) IR provided a significantly higher CNR than FBP, and FIRST-B produced the highest CNR among the 4 methods; (2) FIRST-B provided the highest image quality in the visual evaluation of image noise (speckles and grains) with better interobserver agreement; and (3) FIRST-CS provided the best image quality in the visual evaluation of structure visibility (sharpness and image texture). Maeda et al[15] reported the effect of FIRST on the objective and subjective image quality of coronary vessels on coronary CTA, and they concluded that FIRST improved the image quality even in the setting of a 28% dose reduction. In contrast to their report, we focused on the effects of FIRST on the improvement of image quality and not on the radiation dose reduction. Our study investigated both the main coronary arteries and small branch vessels and plaques, and revealed that the improvement of structure visibility using FIRST-CS was more evident in smaller vessels (i.e., distal vessel and septal branch) than in the proximal vessel. Plaque visualization was also improved with FIRST-CS. Unlike AIDR-3D, FIRST jointly optimizes image quality in both the projection and image spaces.[9] Via the data fidelity component in which the difference evaluation between the original projection and forward-

projected data is performed, FIRST enables high spatial resolution and reduces streak artifacts.[9] Via the noise penalty component with an anatomical-based regularization model, image noise is reduced.[9] The 2 resulting images are combined to produce a new image, leading to a final FIRST image after several iterations. We consider that this process provided better visualization of small vessels and structures (e.g., plaque). Nishida et al[18] compared the image quality of Adamkiewicz artery visualization among FBP, hybrid IR, and model-based IR and found that model-based IR can provide increased CNR and an improved visual score in a small vessel. Their findings are similar to ours, and we believe that model-based algorithms such as FIRST can be especially useful for delineating small vascular structures.

IR can be classified as hybrid or model-based IR, and it effectively reduces image noise on CT imaging.[10,19] The model-based IR provides lower noise and less streak artifacts compared with hybrid IR by considering the optics and system models in addition to the statistical noise model.[20] However, model-based IR has a drawback of a unique blotchy image appearance described as "artificial" or "waxy"[14,20,21] and it is unclear whether spatial resolution with model-based IRs should be preserved in assessing small structures. Our study results illustrated that FIRST-B provided lower visual grading for structure visibility compared with FIRST-CS in the coronary
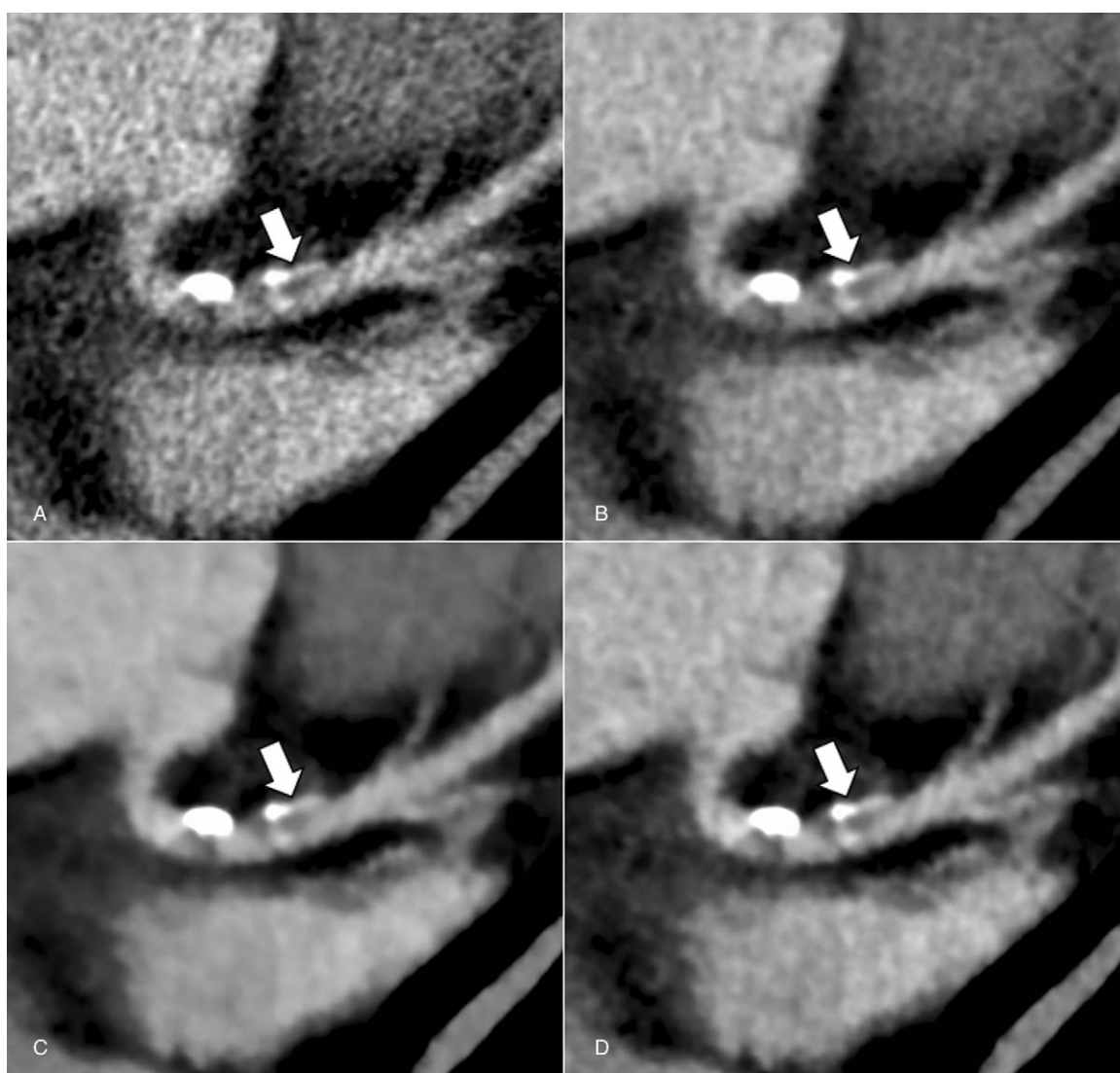
Figure 4. Multiplanar reformation CT angiographic images of partially calcified plaque in the proximal left anterior descending artery (arrows) of a 67-year-old woman under 4 reconstruction algorithms (A, FBP; B, AIDR-3D; C, FIRST-B; and D, FIRST-CS). FIRST images (C and D) show lower noise compared with that of FBP (A) and AIDR-3D images (B). FIRST-CS image (D) shows better plaque visualization with clear margin than the FIRST-B image (C). AIDR-3D = adaptive iterative dose reduction 3D, CNR = contrast-to-noise ratio, CT = computed tomography, D-RCA = distal right coronary artery, FBP = filtered back projection, FIRST-B = forward-projected model-based iterative reconstruction solution–body, FIRST-CS = forward-projected model-based iterative reconstruction solution–cardiac sharp, P-RCA = proximal right coronary artery.

CTA. Katsura et al[20] reported that such an artificial appearance had little effect on the diagnostic acceptability for cervicothoracic lesions, but they evaluated the thyroid gland, common carotid artery, and esophagus, which are relatively large structures. Regarding smaller structures such as coronary arteries and plaques, the artificial appearance might affect the diagnostic capability. We believe that the optimized balance between spatial resolution and image noise behavior achieved by FIRST-CS provided better subjective image quality despite the increased image noise. Jensen et al[13] reported similar results in that the newer model-based IR (Veo 3.0, GE Healthcare) enhanced the imaging evaluation relative to the prior-generation model-based IR (Veo 2.0), and readers awarded higher scores for the imaging appearance of Veo 3.0 despite the increased image noise. These findings suggest that the image noise and image appearance may have a tradeoff relationship. Although artificial image features

were noted, especially in early-generation model-based IR algorithms, recent advances in model-based IR improved the image appearance. We posit that FIRST-CS may provide higher spatial resolution in coronary CTA with acceptable image noise, and it is suitable for the evaluation of CAD. The noise level is one of the important determinants of image quality, but our study results suggested that improved spatial resolution might be more beneficial for the visual evaluation. Tatsugami et al[22] investigated the effect of FIRST-CS on in-stent visualization, and they quantitatively and qualitatively demonstrated that FIRST-CS improved the sharpness of stent visualization with higher spatial resolution.

There were some limitations in our study. First, our study had a single-center, retrospective, and non-randomized design. Small size of the study population was another critical limitation. Multicenter prospective clinical trials in larger population are

needed to validate our data. Second, we did not evaluate diagnostic accuracy by correlating our findings with coronary catheterization findings. Rather, this study aimed to evaluate the image qualities of different reconstruction methods. Further studies should be performed to investigate the effects of the model-based IR on diagnostic capability of CAD. Third, the radiation dose was relatively higher than that used in the prospective study by Stehli et al,[23] who employed a protocol with a low tube voltage (80–100 kV) and tube current (150–210 mA) together with model-based IR (GE Healthcare), whereas our study used a tube voltage and current of 120 kV and 220 to 300 mA, respectively. Also, we employed the cardiac functional analysis mode for the purpose of myocardial motion assessment, and therefore, the radiation dose increased (the mean effective dose, 6.7 ± 3.6 mSv). For the coronary CTA alone, the corresponding radiation dose may be approximately 2 mSv. Lastly, we did not use a low-radiation protocol. Nishiyama et al[24] reported that FIRST had less perceived image noise and better tissue contrast at a similar resolution than AIDR-3D, and it was considered that FIRST might be more advantageous for radiation dose reduction in coronary CTA than AIDR-3D.

In conclusion, FIRST, a new model-based IR algorithm, provides significant improvements in objective and subjective image quality compared with FBP and AIDR-3D. FIRST-B effectively reduces image noise, but the structure visibility of coronary vessels and plaques in FIRST-CS is superior to that in FIRST-B.

Author contributions

Data curation: Kenichiro Hirata, Takeshi Nakaura.

Formal analysis: Kenichiro Hirata, Yoshinori Funama, Seitaro Oda.

Investigation: Kenichiro Hirata, Masafumi Kidoh, Yoshinori Funama, Hideaki Yuki, Yasunori Nagayama, Yuji Iyama, Takeshi Nakaura, Daisuke Sakabe.

Methodology: Daisuke Utsunomiya, Masafumi Kidoh, Takeshi Nakaura, Daisuke Sakabe.

Supervision: Daisuke Utsunomiya.

Writing – original draft: Kenichiro Hirata, Daisuke Utsunomiya.

Writing – review and editing: Daisuke Utsunomiya, Kenichi Tsujita, Yasuyuki Yamashita.

References

[1] Motoyama S, Sarai M, Harigaya H, et al. Computed tomographic angiography characteristics of atherosclerotic plaques subsequently resulting in acute coronary syndrome. J Am Coll Cardiol 2009;54: 49–57.

[2] Cury RC, Abbara S, Achenbach S, et al. CAD-RADS(TM) coronary artery disease - reporting and data system. An expert consensus document of the Society of Cardiovascular Computed Tomography (SCCT), the American College of Radiology (ACR) and the North American Society for Cardiovascular Imaging (NASCI). Endorsed by the American College of Cardiology. J Cardiovasc Comput Tomogr 2016;10:269–81.

[3] Sato A, Aonuma K. Role of cardiac multidetector computed tomography beyond coronary angiography. Circ J 2015;79:712–20.

[4] Nelson RC, Feuerlein S, Boll DT. New iterative reconstruction techniques for cardiovascular computed tomography: how do they work, and what are the advantages and disadvantages? J Cardiovasc Comput Tomogr 2011;5:286–92.

[5] Abdullah KA, McEntee MF, Reed W, et al. Radiation dose and diagnostic image quality associated with iterative reconstruction in coronary CT angiography: a systematic review. J Med Imaging Radiat Oncol 2016;60:459–68.

[6] Oda S, Utsunomiya D, Funama Y, et al. A hybrid iterative reconstruction algorithm that improves the image quality of low-tube-voltage coronary CT angiography. AJR Am J Roentgenol 2012;198:1126–31.

[7] Tumur O, Soon K, Brown F, et al. New scanning technique using adaptive statistical iterative reconstruction (ASIR) significantly reduced the radiation dose of cardiac CT. J Med Imaging Radiat Oncol 2013;57:292–6.

[8] Funama Y, Utsunomiya D, Hirata K, et al. Improved estimation of coronary plaque and luminal attenuation using a vendor-specific model-based iterative reconstruction algorithm in contrast-enhanced CT coronary angiography. Acad Radiol 2017;24:1070–8.

[9] Ohno Y, Yaguchi A, Okazaki T, et al. Comparative evaluation of newly developed model-based and commercially available hybrid-type iterative reconstruction methods and filter back projection method in terms of accuracy of computer-aided volumetry (CADv) for low-dose CT protocols in phantom study. Eur J Radiol 2016;85:1375–82.

[10] Yuki H, Utsunomiya D, Funama Y, et al. Value of knowledge-based iterative model reconstruction in low-kV 256-slice coronary CT angiography. J Cardiovasc Comput Tomogr 2014;8:115–23.

[11] Patino M, Fuentes JM, Hayano K, et al. A quantitative comparison of noise reduction across five commercial (hybrid and model-based) iterative reconstruction techniques: an anthropomorphic phantom study. AJR Am J Roentgenol 2015;204:W176–83.

[12] Paruccini N, Villa R, Pasquali C, et al. Evaluation of a commercial model based iterative reconstruction algorithm in computed tomography. Phys Med 2017;41:58–70.

[13] Jensen CT, Telesmanich ME, Wagner-Bartak NA, et al. Evaluation of abdominal computed tomography image quality using a new version of vendor-specific model-based iterative reconstruction. J Comput Assist Tomogr 2017;41:67–74.

[14] Li G, Liu X, Dodge CT, et al. A noise power spectrum study of a new model-based iterative reconstruction system: Veo 3.0. J Appl Clin Med Phys 2016;17:428–39.

[15] Maeda E, Tomizawa N, Kanno S, et al. The feasibility of Forward-projected model-based Iterative Reconstruction SoluTion (FIRST) for coronary 320-row computed tomography angiography: a pilot study. J Cardiovasc Comput Tomogr 2017;11:40–5.

[16] Millon D, Vlassenbroek A, Van Maanen AG, et al. Low contrast detectability and spatial resolution with model-based Iterative reconstructions of MDCT images: a phantom and cadaveric study. Eur Radiol 2017;27:927–37.

[17] Taylor AJ, Cerqueira M, Hodgson JM, et al. ACCF/SCCT/ACR/AHA/ASE/ASNC/NASCI/SCAI/SCMR 2010 appropriate use criteria for cardiac computed tomography. A report of the American College of Cardiology Foundation appropriate use criteria task force, the Society of Cardiovascular Computed Tomography, the American College of Radiology, the American Heart Association, the American Society of Echocardiography, the American Society of Nuclear Cardiology, the North American Society for Cardiovascular Imaging, the Society for Cardiovascular Angiography and Interventions, and the Society for Cardiovascular Magnetic Resonance. J Cardiovasc Comput Tomogr 2010;4:407.e1–33.

[18] Nishida J, Kitagawa K, Nagata M, et al. Model-based iterative reconstruction for multi-detector row CT assessment of the Adamkiewicz artery. Radiology 2014;270:282–91.

[19] Yin WH, Lu B, Li N, et al. Iterative reconstruction to preserve image quality and diagnostic accuracy at reduced radiation dose in coronary CT angiography: an intraindividual comparison. JACC Cardiovasc Imaging 2013;6:1239–49.

[20] Katsura M, Sato J, Akahane M, et al. Comparison of pure and hybrid iterative reconstruction techniques with conventional filtered back projection: image quality assessment in the cervicothoracic region. Eur J Radiol 2013;82:356–60.

[21] Kligerman S, Lahiji K, Weihe E, et al. Detection of pulmonary embolism on computed tomography: improvement using a model-based iterative reconstruction algorithm compared with filtered back projection and iterative reconstruction algorithms. J Thorac Imaging 2015;30:60–8.

[22] Tatsugami F, Higaki T, Sakane H, et al. Coronary artery stent evaluation with model-based iterative reconstruction at coronary CT angiography. Acad Radiol 2017;24:975–81.

[23] Stehli J, Fuchs TA, Bull S, et al. Accuracy of coronary CT angiography using a submillisievert fraction of radiation exposure: comparison with invasive coronary angiography. J Am Coll Cardiol 2014;64:772–80.

[24] Nishiyama Y, Tada K, Nishiyama Y, et al. Effect of the forward-projected model-based iterative reconstruction solution algorithm on image quality and radiation dose in pediatric cardiac computed tomography. Pediatr Radiol 2016;46:1663–70.